Journal of Chromatography, 607 (1992) 79–89
Elsevier Science Publishers B.V., Amsterdam

CHROM. 24 278

Efficiency in supercritical fluid chromatography as a function of linear velocity, pressure/density, temperature and diffusion coefficient employing *n*-pentane as the eluent

A. Hütz and E. Klesper

Lehrstuhl für Makromolekulare Chemie, Aachen University of Technology, Worringerweg 1, D(W)-5100 Aachen (Germany)

(First received January 22nd, 1992; revised manuscript received April 22nd, 1992)

ABSTRACT

The effect of the physical factors linear velocity, pressure/density, and temperature on the efficiency expressed in terms of effective plate number, N_{eff}, or height equivalent to a theoretical plate, H_{eff}, were studied for supercritical fluid chromatography using *n*-pentane as the mobile phase modified with a small amount of methanol (0.5%, v/v), unbonded silica gel as the stationary phase, and a mixture of polycyclic aromatic hydrocarbons as the analytes on a packed analytical column (4.6 mm I.D.). The results are presented as three-dimensional graphs which, on plotting N_{eff} of chrysene, N_{eff}(C), *versus* column average pressure, $\bar{p}$, and temperature, T, at different constant linear velocities, $\bar{u}$, show movement of the maxima of N_{eff} to higher temperatures when $\bar{u}$ increases. Moreover, the maxima are highest at medium $\bar{u}$, *i.e.*, at $\bar{u}_{opt}$. An analogous behaviour is found when N_{eff}(C) is plotted *versus* the average density in the column, $\bar{\rho}$. On replacing N_{eff}(C) with the capacity factor of chrysene, k'(C), and again plotting *versus* $\bar{p}$ and T, the k'(C) values do not change greatly with increasing $\bar{u}$. If the customary Van Deemter plots of H_{eff}(C) *versus* $\bar{u}$ are combined with $\bar{p}$ or $\bar{\rho}$ as a third axis, keeping T = constant, the dependence of $\bar{u}_{opt}$ on $\bar{p}$ or $\bar{\rho}$ becomes obvious. As expected, $\bar{p}$ and $\bar{\rho}$ should be kept as low as possible in order to obtain low H_{eff}(C). Employing T as the third dimension for the Van Deemter plots and keeping p = constant, it is seen that only specific ranges of T yield the low H_{eff}(C). The graphs are explained in terms of the interdiffusion coefficient, $D_{1,2}$. Three-dimensional graphs for the dependence of $D_{1,2}$ or of the viscosity on pressure and temperature are shown. The three-dimensional plots of N_{eff}(C) and H_{eff}(C) can be rationalized with respect to their dependence on the average linear velocity, pressure/density and temperature.

INTRODUCTION

In supercritical fluid chromatography (SFC) many and, in part, very early studies have been reported on the dependence of the capacity factor, k', and the selectivity, α, on pressure/density, p/ρ, or on temperature, T, for different single mobile phases, stationary phases and analytes (*e.g.*, [1–10]). Many studies are also concerned with k' and α for binary mobile phases (*e.g.*, [11–18]). There are, in addition, a number of reports dealing with the dependence of the efficiency, either in terms of plate numbers, N, or of height equivalent to a theoretical plate, H, and with the dependence of the resolution, R, on pressure/density and on temperature [2,4,5,8, 10,16–23]. In a number of these studies, particularly with packed columns, the volume flow-rate of the pump, and therefore approximately the mass flow-rate, was kept constant during the measurement of a chromatogram. In other studies, particularly with microcolumns, the volume flow-rate of the pump was changed to obtain some desired pressure or density. Therefore, with both packed columns and microcolumns, the linear velocity of the mobile phase in the column was not constant during a separation and hence was not changed in a way generally suitable for optimizing this velocity with the aim of optimizing the chromatographic parameters. Moreover, the dependence of the chromatographic parameters on the average linear velocity, $\bar{u}$,

Correspondence to: Dr. E. Klesper, Lehrstuhl für Makromolekulare Chemie, Aachen University of Technology, Worringerweg 1, D(W)-5100 Aachen, Germany.

0021-9673/92/$05.00 © 1992 Elsevier Science Publishers B.V. All rights reserved

has not received sufficient attention in publications, although the velocity should be considered more closely on account of its large influence on the chromatographic parameters [8,10,24–28]. The linear velocity in conjunction with the dynamic viscosity, η, of the mobile phase also determines the pressure drop, Δp, over a given column which, in turn, may influence the chromatographic parameter s by means of solubility and peak compression. Often lacking in previous work is a systematic investigation of the simultaneous influence of all independent physical parameters of the mobile phase on the chromatographic parameters. Because of the large experimental effort required for this type of study, it may be practical only for some selected and typical chromatographic system. This is even more the case if it is considered that, for obtaining a complete set of information, the stationary phase should also be changed over an appropriate range of physical and chemical properties. The same applies to the chemical nature of the substrate.

In this work, the influence of the average linear velocity, pressure/density and temperature on efficiency and retention was simultaneously studied for a specific chromatographic system. The system consisted on *n*-pentane as the mobile phase, unbonded silica gel as the stationary phase, a mixture of four polycyclic aromatic hydrocarbons as the analytes and an analytical wide-bore (4.6 mm I.D.) packed column. The influence of the four physical properties $\bar{u}$, p/ρ and T on the three chromatographic parameters effective plate number, N_{eff}, effective plate height, H_{eff}, and capacity factor, k', is presented in the form of three-dimensional graphs and explained by the interdiffusion coefficients. The graphs allow an immediate overview of the interrelations between physical and chromatographic parameters. The influence of $\bar{u}$, p/ρ and T on the chromatographic parameters resolution, R, and capacity factor, k', for the same chromatographic system will be the subject of a forthcoming paper [29].

In this and in previous studies (*e.g.*, [8–10,21]) the chromatographic experiments were standardized to simplify comparisons. First, the standardization applies to the stationary phase for which unbonded (naked) silica gel was used because this is both the simplest and an often employed phase which was (and still is to some extent) more stable toward temperature and solvolysis than many bonded phases. The polycyclic aromatic hydrocarbons used as the analytes are also employed by many investigators and range from those possessing considerable vapour pressure at the temperatures at which the chromatography is carried out to those with only a low vapour pressure. When there is no or negligible vapour pressure, movement through the column is due only to the dissolution power of the mobile phase. In this work with naphthalene, anthracene, pyrene and chrysene as the analytes and *n*-pentane as the mobile phase, some vapour pressure exists even for chrysene because separations with this mobile phase required temperatures up to 300°C. Another standardization applied to the feed rate of the pump and the column with a length of 25 cm and an I.D. of 4.6 mm. Either a constant pump feed rate of 1 ml min^{-1} at ambient temperature in the liquid state was chosen, or else, as in this work, a varied pump feed rate which was adjusted to yield a constant average linear velocity in the separation column. A constant pump feed rate has the advantage of being conveniently obtainable with simple present-day hardware. Specifically, the rate of 1 ml min^{-1} is in the general range of $\bar{u}_{\text{opt}}$ with the present mobile phase and column (bare silica gel; 4.6 mm I.D.) whereby it is to be understood that $\bar{u}_{\text{opt}}$ depends on the nature of the mobile phase, stationary phase, p and T.

EXPERIMENTAL

The eluent, *n*-pentane, containing a small amount of the modifier methanol (0.5%, v/v), was supplied from a container pressurized by helium. Between the container and a piston-driven membrane pump (Type MF 65; Orlita, Germany) a filter of stainless-steel frits (2-μm pore size) and between the pump and the column a membrane-type pulse damper (Type 3.350; Orlita) were installed. The analytical column (25 cm × 0.46 cm I.D.) was packed with unbonded silica gel (LiChrosorb Si 100, 10 μm; Merck, Germany) using a slurry method, the column being placed in an air-circulated oven (Type UT 5042, Heraeus, Germany). The column inlet and outlet pressures were measured with Bourdon-type manometers (class 0.6 VDO; Wika, Germany). For each chromatogram, 20 μl of a sample solution of naphthalene, anthracene, pyrene and chrysene, dis-

solved in *n*-heptane (0.13, 0.07, 0.13 and 0.03 mg, respectively, in 1 ml of heptane), were introduced by a loop injector (Type 7125; Rheodyne, USA) and monitored at the column exit by a UV detector (Type LC-75; Perkin-Elmer, USA). The outlet pressure downstream of column and detector was controlled by an adjustable back-pressure valve (Type 26-3200; Tescom, USA). To measure the flow-rate, the eluted mobile phase was collected with cooling. The apparent average linear velocity in the column was determined using $\bar{u} = L/t_0$ (L = column length, t_0 = dead time), whereby an injection of *n*-heptane was employed to determine t_0.

The four polycyclic aromatic hydrocarbons were purified by crystallization or sublimation. The *n*-pentane was dried over sodium, distilled, filtered and degassed. The methanol used as the modifier was of spectroscopic grade. The effective plate number, N_{eff}, and the effective plate height, H_{eff}, were obtained from the chromatogram according to

$$N_{eff} = 5.54\,(t'_r/w')^2 \quad (1)$$

and

$$H_{eff} = L/N_{eff} \quad (2)$$

where $t'_r = t_r - t_0$ is the net retention time, t_r the retention time, w' the width of the peak at half-height and L the column length. The capacity factors were obtained from $k' = (t_r - t_0)/t_0$.

For collecting chromatographic data, the physical parameters for the necessary isobaric–isothermal runs at constant linear velocity were varied between chromatograms as follows: at a given constant temperature, chromatograms were obtained for each average linear velocity and for each average pressure, whereby only one of the two physical parameters was changed at a time. Then the temperature was changed and enough time was allowed for the system to reach equilibrium before the velocity and pressure were changed in steps again. In all, chromatograms were obtained from 210 to 300°C and at apparent average velocities from 0.1 to 0.5 cm s^{-1} and at pressures from 20 to 70 bar.

Most of the N_{eff} data thus obtained correspond to a regular data grid of pressure and temperature, at a given constant linear velocity. Another part of the data, which were not obtained at regular intervals of pressure or density, and therefore did not fit the desired regular grid, were first drawn as curves *versus* pressure or density and then interpolated to obtain data which conformed to the grid. All the N_{eff} data were then used to calculate also the H_{eff} according to eqn. 2. Fig. 1a shows the directly measured lines of the pressure–temperature grid (solid lines) and the lines obtained by interpolation (dashed lines), whereby the pressures are average column pressures $\bar{p} = (p_i + p_o)/2$ (i, o = inlet and outlet, respectively). From theoretical considerations it is known that the arithmetic mean pressure $\bar{p}$ is about two thirds of the way down the column and is only reached after about two thirds of the total residence time of the mobile phase in the column [30]. The p–T pairs were converted into ρ–T pairs using published tables [31,32]. The calculations assumed pure *n*-pentane, neglecting the effect of the

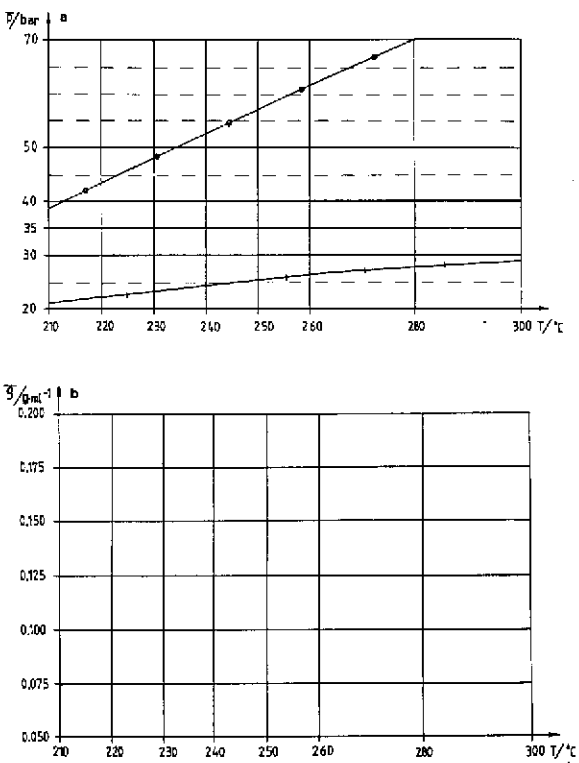

Fig. 1. (a) Two-dimensional grid of direct and interpolated experimental data (*e.g.*, of effective plate number, N_{eff}, or of capacity factor, k') at average column pressures, $\bar{p}$, temperatures, T, and constant average linear velocity. Sloping lines represent isochores of (+) $\rho = 0.050$ g cm^{-3} and (○) $\rho = 0.200$ g cm^{-3}. (b) Two-dimensional grid of experimental data (*e.g.*, N_{eff} or k') at average densities in the column, $\bar{\rho}$, temperatures, T, and constant average linear velocity. Grid is derived from the $\bar{p}$–T data in (a).

0.5% (v/v) modifying methanol on density. The density–temperature grid derived in this way from the original pressure–temperature grid in Fig. 1a is shown in Fig. 1b; the densities, $\bar{\rho}$, are average column densities corresponding to the average column pressures, $\bar{p}$. The isochores at the highest (0.20 g cm^{-3}) and the lowest density (0.05 g cm^{-3}) occurring in Fig. 1b are seen as two sloping lines in Fig. 1a. In order to obtain for Fig. 1b a rectangular grid, essentially only those data of Fig. 1a which are situated between the two isochores appear in Fig. 1b. Therefore, Fig. 1b contains less data than Fig. 1a and the same applies to plots seen later which show $\bar{\rho}$ instead of $\bar{p}$. For each average linear velocity a separate grid is established both for the type of grid in Fig. 1a and that in Fig. 1b. Each intersection or tee in Fig. 1a and b represents one data point for one of the chromatographic parameters (N_{eff}, H_{eff} or k'). From the grids three-dimensional graphs were obtained using a personal computer and graphics software as described previously [33].

RESULTS AND DISCUSSION

The data for N_{eff} are plotted as the third axis in three-dimensional plots and also as the hatching of the three-dimensional surfaces in these plots in Figs. 2 and 3. In Fig. 2a, b and c the other two axes are $\bar{p}$ and T and in Fig. 3a, b and c they are $\bar{\rho}$ and T, with the linear velocity, $\bar{u}$, being kept constant for a given plot. From the five linear velocities actually employed ($\bar{u}$ = 0.1, 0.2, 0.3, 0.4 and 0.5 cm s^{-1}), only three ($\bar{u}$ = 0.1, 0.3 and 0.5 cm s^{-1}) are shown in Figs. 2 and 3. Moreover, only the N_{eff} for chrysene, N_{eff}(C), is shown, chrysene being the last-eluting analyte in the mixture of polycyclic aromatic hydrocarbons used as a test substrate. Remarkably, all the plots presented in Figs. 2 and 3 are of similar shape, at least in principle. Particularly at a given low pressure or at a given low density, N_{eff}(C) passes through pronounced maxima with changing temperature. When the pressure increases, the maxima are found at higher temperatures than at lower pressures (Fig. 2). However, when the density increases this effect is hardly present any longer (Fig. 3). In both instances, the maxima decrease strongly in height with increasing pressure or increasing density. With increasingly linear velocity, *i.e.*, going from a to b to c, the maxima are shifted to higher

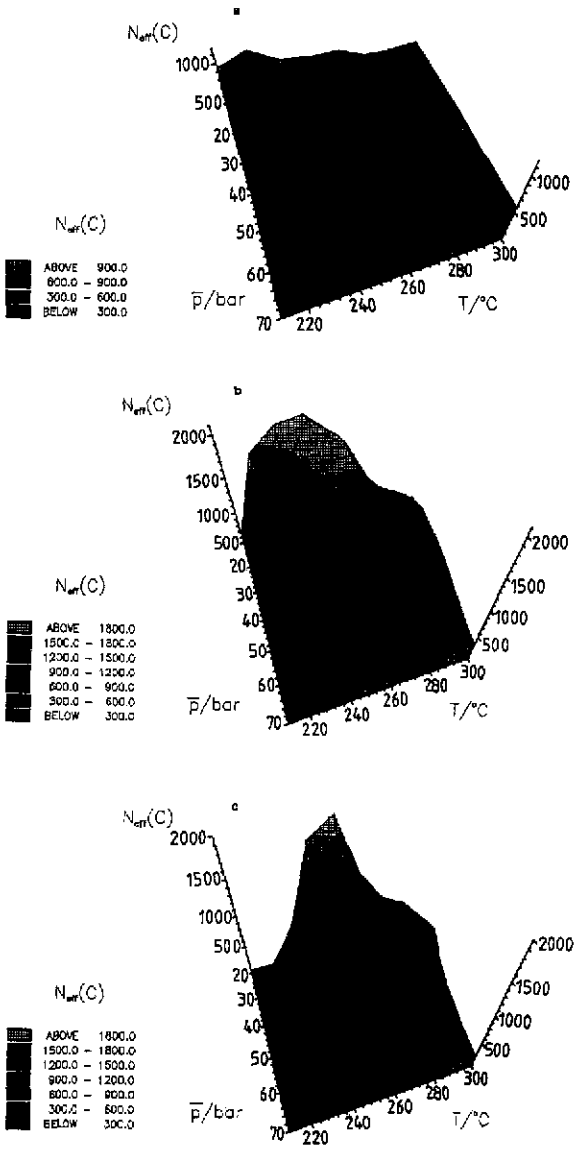

Fig. 2. Effective plate numbers of chrysene, N_{eff}(C), *versus* average column pressure, $\bar{p}$, and temperature, T, at three constant average linear velocities, $\bar{u}$: (a) 0.1; (b) 0.3; (c) 0.5 cm s^{-1}. The N_{eff}(C) are plotted on the z-axis as a three-dimensional surface, but they are also indicated as shadings on the surface of the graph. The data were obtained with *n*-pentane as mobile phase and unbonded silica gel as stationary phase.

temperatures. Thereby, the heights of the maxima appear to reach their greatest height at some intermediative velocity. With increasing velocity, the areas of low N_{eff}(C) become larger. Therefore, it becomes less easy to select $\bar{p}$–T or $\bar{\rho}$–T regions

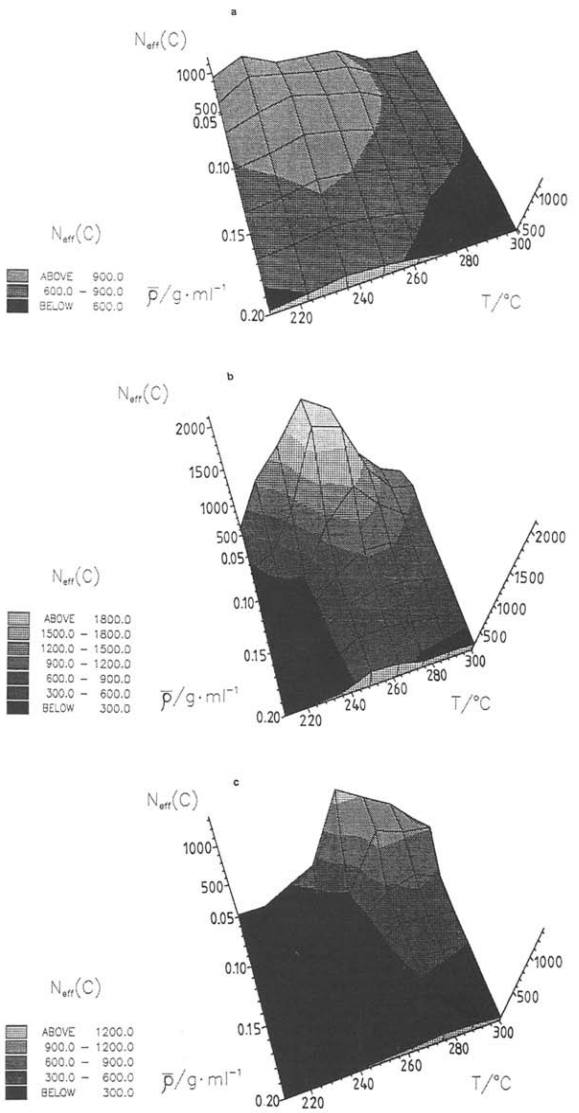

Fig. 3. Effective plate numbers of chrysene, $N_{eff}(C)$, *versus* average density of the mobile phase in the column, $\bar{\rho}$, and temperature, T, at three constant average linear velocities, $\bar{u}$: (a) 0.1; (b) 0.3; (c) 0.5 cm s^{-1}. Other details as in Fig. 2.

possessing an acceptable $N_{eff}(C)$ at higher than at lower velocity. Summarizing, in Figs. 2 and 3 strong decreases in $N_{eff}(C)$ from their maxima are seen when proceeding to higher pressures and higher or lower temperatures. Also, the highest $N_{eff}(C)$ are obtained at medium velocities in Figs. 2 and 3, which are closer to the optima of the velocity, $\bar{u}_{opt}$.

The results in Figs. 2 and 3 may be qualitatively explained by the Van Deemter equation and its modifications [34,35]:

$$H = A + B/\bar{u} + C\bar{u} + D\bar{u} \tag{3}$$

with H_{eff} being derived from H by

$$H \cdot \frac{(1 + k')^2}{k'^2} = H_{eff} \tag{4}$$

and

$$A = 2\lambda d_p \tag{5}$$

$$B = 2\gamma D_{1,2} = B' D_{1,2} \tag{6}$$

$$C = \frac{\Theta(k_0 + k' + k_0 k')^2 d_p^2}{30 k_0 (1 + k_0)^2 (1 + k')^2 D_{1,2}} = \\ = \frac{C'(k_0 + k' + k_0 k')^2}{D_{1,2} k_0 (1 + k_0)^2 (1 + k')^2} = \frac{C''}{D_{1,2}} \tag{7}$$

$$D = \frac{2k'}{(1 + k_0)(1 + k')^2 k_d} = \frac{D'}{k_d} \tag{8}$$

where

- λ = eddy diffusion factor for the dispersion of size, direction, and velocity of the mobile phase streams in the interstitial flow channels between particles;
- γ = obstruction factor for longitudinal diffusion;
- Θ = tortuosity factor for impeding the diffusion within the intraparticulate pores of the particles;
- k_0 = ratio of the intraparticulate void volume to the interstitial void volume;
- k_d = velocity constant of desorption of analyte from the outside surface and from the pore surface of the particles;
- $D_{1,2}$ = interdiffusion coefficient of the analyte molecules in the mobile phase.

λ, γ and Θ may be tentatively considered as independent of $\bar{p}$, T and $\bar{u}$ for a given chromatographic system, *i.e.*, for a given mobile and stationary phase, column geometry and analyte. The same may apply to k_0, but k', k_d and $D_{1,2}$ will depend strongly on p and T, although not on $\bar{u}$. It should be noted, however, that it may be expected that with greatly increasing $\bar{u}$ the pressure drop along the column, Δp, may reach levels such that k', k_d, and

$D_{1,2}$ start to depend to a considerable extent on $\bar{u}$ via Δp. This may arise if k', for instance, in the first half of the column decreases considerably less on account of higher density than it will increase in the second half of the column owing to lower density.

Turning now to the capacity factor instead of N_{eff}, the behaviour of the capacity factor of chrysene, $k'(C)$, with respect to $\bar{p}$, T and $\bar{u}$ can be seen in the plots in Fig. 4. There is the usual strong decrease in k' with increasing $\bar{p}$ and also with increasing T, provided that one has passed already the maximum value of k' as a function of T, as is the case here. At velocities $\bar{u}$ between 0.1 and 0.4 cm s^{-1} little if any change in k' with $\bar{u}$ can be observed, but some decrease in k' may, in fact, be present with $\bar{u} = 0.5$ cm s^{-1} at low $\bar{p}$ and T. On the whole, and over a moderate range of $\bar{u}$, one finds a k' which depends strongly on $\bar{p}$ and T but not on $\bar{u}$. If one desires to quantify the behaviour of k' it should be considered that a pressure drop over the column changes the k' along the column. One may start with the concept of an infinite number of equally long, identical sections over the total column length, each of these sections having its own k'. If there exists a significant pressure drop Δp at T = constant along the column, for instance, the sections closer to the inlet of the column will exhibit a lower k', whereas the sections closer to the outlet of the column will show a larger k', all relative to the k' measured experimentally for the total column length. This total k' will be composed of the k' of the individual sections. Assuming for simplicity that the total column is composed of only three sections, 1, 2 and 3, of equal length, one may start from the additivity of the retention times:

$$t_{r,1} + t_{r,2} + t_{r,3} = t_r(\text{total}) \quad (9)$$

where $t_{r,i}$ is the retention time of the analyte in the ith section. Similarly, one may write for the corresponding dead times

$$t_{0,1} + t_{0,2} + t_{0,3} = t_0(\text{total}) \quad (10)$$

If the same p–T conditions exist for all sections of the column,

$$t_{r,1} = t_{r,2} = t_{r,3} = 1/3\, t_r(\text{total}) \quad (11)$$

$$t_{0,1} = t_{0,2} = t_{0,3} = 1/3\, t_0(\text{total}) \quad (12)$$

If the p–T conditions are different, then eqns. 11 and 12 do not hold. Subtracting eqn. 10 from eqn. 9 and dividing by eqn. 10 yields

$$\frac{t_{r,1} - t_{0,1}}{t_{0,1} + t_{0,2} + t_{0,3}} + \frac{t_{r,2} - t_{0,2}}{t_{0,1} + t_{0,2} + t_{0,3}} + \frac{t_{r,3} - t_{0,3}}{t_{0,1} + t_{0,2} + t_{0,3}} = \frac{t_r(\text{total}) - t_0(\text{total})}{t_0(\text{total})} = k'(\text{total}) \quad (13)$$

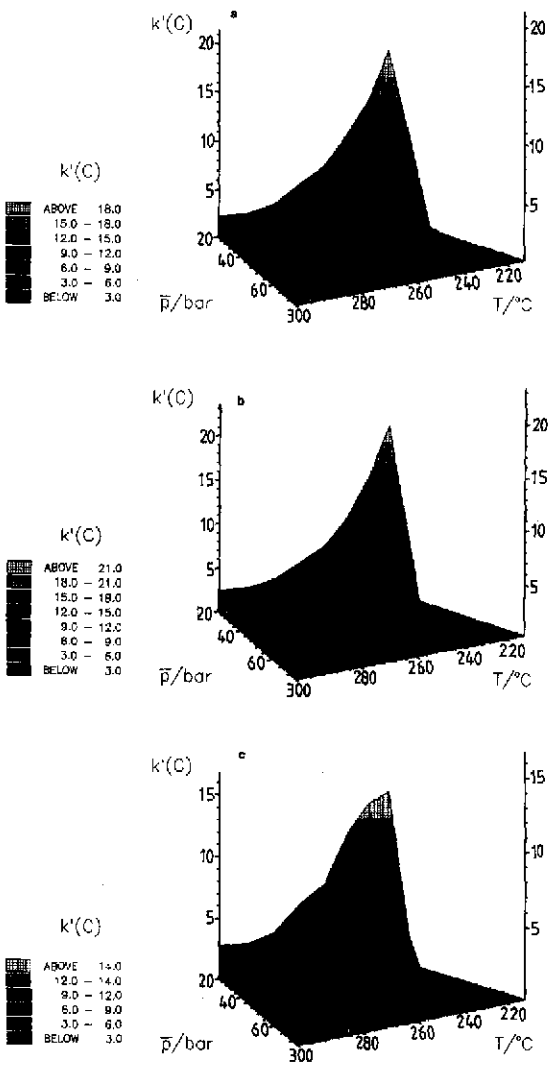

Fig. 4. Capacity factors of chrysene, $k'(C)$, *versus* average column pressure, $\bar{p}$, and temperature, T, at three constant average linear velocities, $\bar{u}$: (a) 0.1; (b) 0.3; (c) 0.5 cm s^{-1}. The $k'(C)$ are plotted on the z-axis as a three-dimensional surface and also shown by shading of this surface.

Considering that the density will be proportional to the dead time, provided that the mass flow-rate is not changed, it is obvious that the $t_{0,i}$ can be transformed into each other by a ratio of densities:

$$t_{0,1} = (\rho_1/\rho_2)t_{0,2} \quad (14a)$$

$$t_{0,1} = (\rho_1/\rho_3)t_{0,3} \quad (14b)$$

$$t_{0,2} = (\rho_2/\rho_3)t_{0,3} \quad (14c)$$

where the ρ_i are the densities in the ith section of the column, as counted from the column inlet. Substitution of eqns. 14 in eqn. 13 leads to

$$\frac{t_{r,1} - t_{0,1}}{(1 + \rho_2/\rho_1 + \rho_3/\rho_1)t_{0,1}} + \frac{t_{r,2} - t_{0,2}}{(\rho_1/\rho_2 + 1 + \rho_3/\rho_2)t_{0,2}} + \frac{t_{r,3} - t_{0,3}}{(\rho_1/\rho_3 + \rho_2/\rho_3 + 1)t_{0,3}} = k'(\text{total}) \quad (15)$$

or

$$\frac{k'_1}{1 + \rho_2/\rho_1 + \rho_3/\rho_1} + \frac{k'_2}{\rho_1/\rho_2 + 1 + \rho_3/\rho_2} + \frac{k'_3}{\rho_1/\rho_3 + \rho_2/\rho_3 + 1} = k'(\text{total}) \quad (16)$$

whereby the denominators with their ρ_i can be considered as weighting factors for the k' in the individual sections. Eqn. 13 can be generalized for n column sections, as in fact has been written before [36]:

$$\frac{\sum_{i=1}^{n} t_{r,i} - \sum_{i=1}^{n} t_{0,i}}{\sum_{i=1}^{n} t_{0,i}} = \frac{\sum_{i=1}^{n} (t_{0,i}k'_i)}{\sum_{i=1}^{n} t_{0,i}} = k'(\text{total}) \quad (17)$$

Eqn. 16 can also be rewritten as

$$\frac{k'_1}{\frac{\rho_1 + \rho_2 + \rho_3}{\rho_1}} + \frac{k'_2}{\frac{\rho_1 + \rho_2 + \rho_3}{\rho_2}} + \frac{k'_3}{\frac{\rho_1 + \rho_2 + \rho_3}{\rho_3}} = k'(\text{total}) \quad (18)$$

which becomes in general

$$\frac{\sum_{i=1}^{n} (k'_i\rho_i)}{\sum_{i=1}^{n} \rho_i} = \frac{\sum_{i=1}^{n} \frac{k'_i}{u_i}}{\sum_{i=1}^{n} \frac{1}{u_i}} = k'(\text{total}) \quad (19)$$

where u_i is the linear velocity in the ith column section. The u_i are inversely proportional to the ρ_i, other conditions being equal.

Inspecting Fig. 5, where the experimental pressure drop Δp is plotted *versus* $\bar{p}$ and T at $\bar{u}$ = constant, the expected strong decrease in Δp with decreasing $\bar{u}$ is seen. In fact, a graph for $\bar{u} = 0.1$ cm s^{-1} is not shown in Fig. 5 on account of the small Δp, leading with our experimental set-up to large relative errors in measurement. However, one can conclude from the data that Δp at $\bar{u} = 0.1$ cm s^{-1} is too small to cause significant differences between the k'_i along the column. Therefore, one may take the results of k'(total) in Fig. 4a ($\bar{u} = 0.1$ cm s^{-1}) as the results one will obtain not only at some average $\bar{p}$ but also at $\bar{p}$ = p(inlet) = p(outlet), *i.e.*, $\Delta p = 0$, that is, without pressure drop over the entire column. One may then read the approximate k'_i for individual sections of the column which possess different p from Fig. 4a. Assuming higher Δp, it is seen from Fig. 4a, b and c that the k'_i of the sections of the first

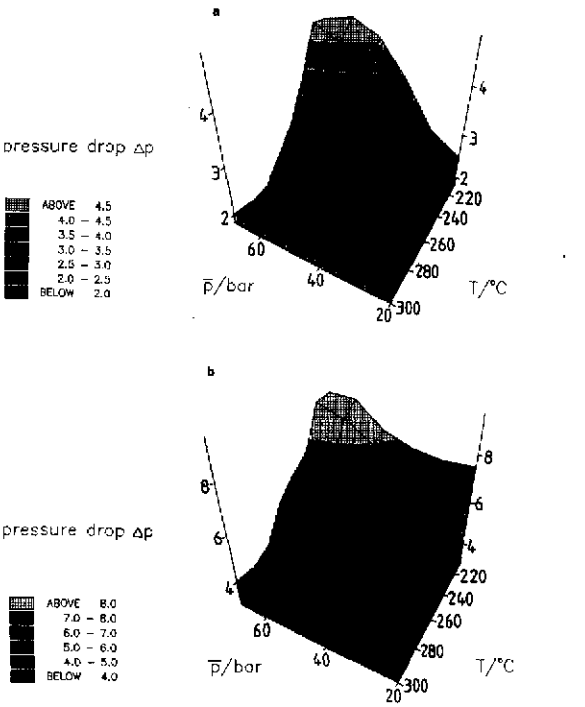

Fig. 5. Pressure drop over the total column, Δp (bar), *versus* average column pressure, $\bar{p}$, and temperature, T, at two constant velocities, $\bar{u}$: (a) 0.3; (b) 0.5 cm s^{-1}. The Δp are presented both on the z-axis and by shading.

half of the column will be compensated in part by the k_i' of the second half. This is the case whenever the k_i' of a p(inlet) is connected to the k_i' of p(outlet) by a sloping, more or less straight line in the graph. One may expect that within the range of the present pressure drops Δp, the k'(total) are roughly independent of $\bar{u}$, as in fact is found experimentally.

The p–T dependence of the interdiffusion coefficient $D_{1,2}^{\circ}$ at infinite dilution for chrysene in n-pentane is presented in Fig. 6, together with the viscosity data [37] needed for its calculation. The $D_{1,2}^{\circ}$ values were calculated according to the Wilke–Chang equation [38]:

$$D_{1,2}^{\circ} = 7.4 \cdot 10^{-8} \frac{(\phi M_2)^{\frac{1}{2}} T}{\eta_2 V_1^{0.6}} = K \cdot \frac{T}{\eta_2} \qquad (20)$$

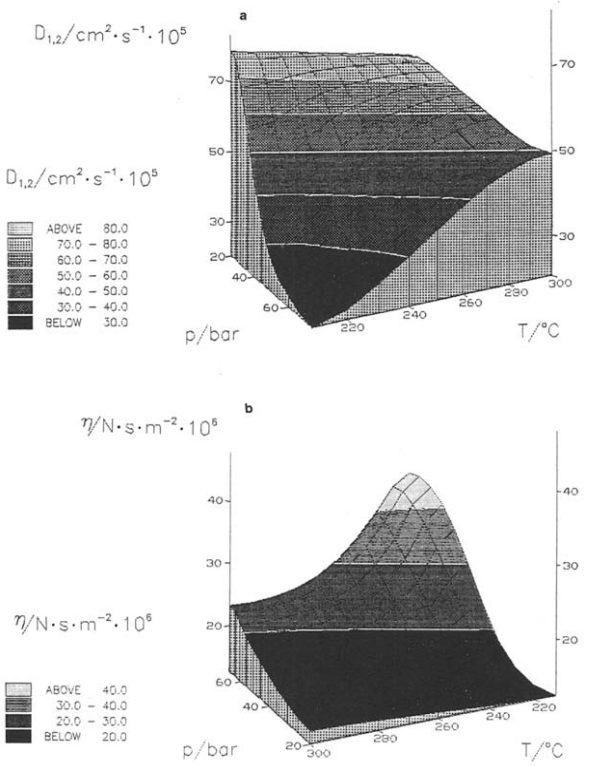

Fig. 6. (a) Interdiffusion coefficient, $D_{1,2}$, of chrysene in n-pentane at different pressures, p, and temperatures, T. $D_{1,2}$ calculated by the Wilke–Chang equation. Data are presented both on the z-axis and by shading. (b) Dynamic viscosity, η, of n-pentane at different pressures, p, and temperatures, T. Data are presented both on the z-axis and by shading.

where 1 and 2 refer to the analyte and the supercritical fluid, respectively, ϕ = dimensionless association factor (1.0 for unassociated supercritical fluids such as n-pentane), M_2 = molecular weight of the fluid, η_2 = dynamic viscosity of the fluid (cP), V_1 = molar volume of the analyte at its normal boiling temperature (cm^3 g mol^{-1}) and K the combination of constants which is valid for a given solvent and solute. Although the Wilke–Chang equation is intended for liquid solvents, it is expected to yield reasonable values also for dense supercritical fluids well above T_c. The η_2 in Fig. 6b follow expectations in as much as an increasing pressure increases the viscosity particularly at lower temperature. It may be noted in passing that at a given density the temperature has only a negligible influence on viscosity [38], which means that lines of equal η in Fig. 6b have p–T pairs that lead to equal ρ.

The interdiffusion coefficient $D_{1,2}$ in Fig. 6a shows, as expected, a pronounced drop at the highest pressure and lowest temperature. This is also the location of highest η_2, the η_2 exerting a larger influence than temperature on $D_{1,2}$ (eqn. 20) because the relative ranges studied here are larger for η than for T. Obviously, a large $D_{1,2}$ may be obtained at low pressure over the entire temperature range. To obtain a sizeable $D_{1,2}$ at higher pressures, however, a higher temperature is required.

The viscosity, η, is not only connected to $D_{1,2}$ but also to the pressure drop, Δp. The viscosity and the average linear velocity, $\bar{u}$, of the fluid are the variables to determine the pressure drop for a given chromatographic column. According to Darcy's law,

$$\frac{dp}{dx} = -\frac{\bar{u}\eta}{B} \qquad (21)$$

where B is the specific permeability coefficient of a given column. Because $\bar{u}$ and η are in general functions of the distance travelled in the column, x, eqn. 21 is written in differential form. The experimental column pressure drop, Δp, in Fig. 5 increases with η and $\bar{u}$, as expected, although a non-trivial dp/dx must actually hold because of non-linear functions $u(x)$ and $\eta(x)$, and possibly also on account of partially non-laminar flow.

Plotting H_{eff} *versus* $\bar{u}$ at constant pressure and temperature would yield Van Deemter-type graphs.

In Figs. 7a, b and c pressure or density is employed as an additional third axis, showing the Van Deemter plots of H_{eff} of chrysene, $H_{eff}(C)$, as a function of $\bar{p}$ or $\bar{\rho}$ at T = constant. In Fig. 7a, which present the Van Deemter plot as a function of $\bar{p}$ at T = 220°C, the location of $\bar{u}_{opt}$ is shown as the dark black area. The movement of $\bar{u}_{opt}$ to lower $\bar{u}$ with increasing pressure becomes obvious, in addition to the very unfavourable $H_{eff}(C)$ with larger $\bar{u}$, *i.e.*, on the high velocity part of the graph. When the temperature is raised to 280°C, other conditions being equal, as in Fig. 7b, the higher temperature yields in almost all areas of the graph lower H_{eff} than in Fig. 7a. When $\bar{\rho}$ is used as the third axis instead of $\bar{p}$, T remaining at 280°C, as in Fig. 7c, the graph remains similar to Fig. 7b. Again, the $\bar{u}_{opt}$ move to lower $\bar{u}$ as pressure or density is increased, whereby at the highest pressure and densities the $H_{eff}(C)$ apparently have left the useful range. Fig. 8 shows the dependence of the Van Deemter plots on temperature at a constant pressure of p = 30 bar (Fig. 8a) and 50 bar (Fig. 8b). There is a tendency for $\bar{u}_{opt}$

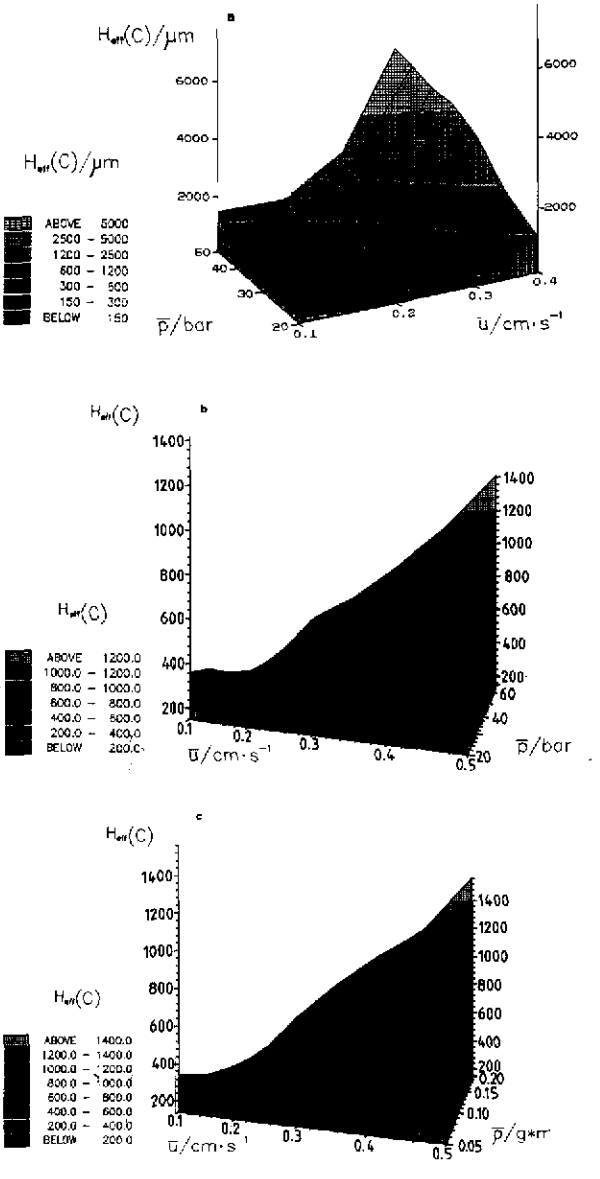

Fig. 7. (a) Effective plate height of chrysene, $H_{eff}(C)$, as a function of average linear velocity, $\bar{u}$, and average column pressure, $\bar{p}$, at 220°C. This is a Van Deemter-type plot with the additional feature of exhibiting the dependence on $\bar{p}$ on a third axis. (b) As (a), but at 280°C. (c) As (b), but replacing $\bar{p}$ with the average density, $\bar{\rho}$.

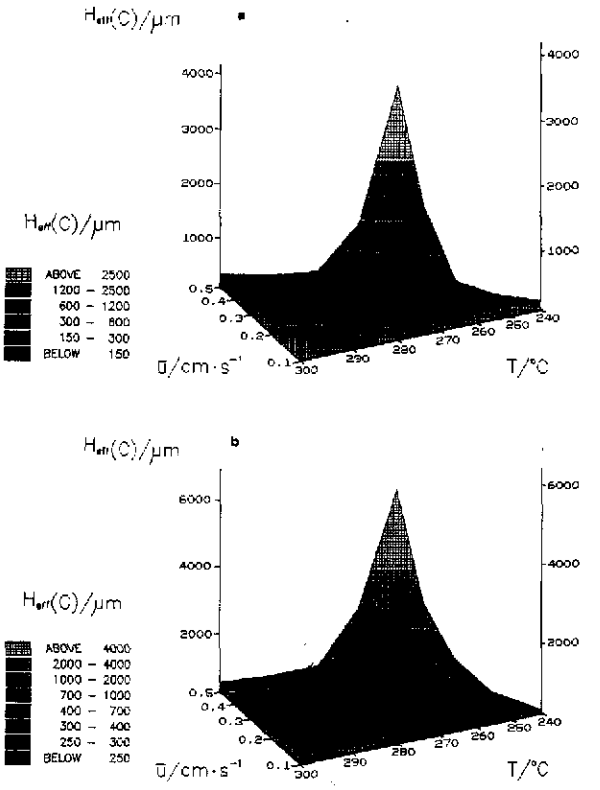

Fig. 8. Effective plate height of chrysene, $H_{eff}(C)$, as a function of average linear velocity, $\bar{u}$, and temperature, T, at a constant pressure. This is a Van Deemter-type plot with the additional feature of exhibiting the temperature dependence on a third axis. $\bar{p}$ = (a) 30 and (b) 50 bar.

to move to higher $\bar{u}$ when the temperature is raised. Comparing Fig. 8a and b, the range of $\bar{u}_{opt}$ is located at higher velocities when the pressures are lower and the H_{eff} are generally smaller. Both Figs. 7 and 8 lead to analogous conclusions.

The appearance of a minimum in H or H_{eff} at $\bar{u}_{opt}$ is, of course, a consequence of the validity of Van Deemter-type equations such as eqn. 3. Because the A term in eqn. 3 does not usually change much with $\bar{u}$ in gas chromatography, it is taken in eqn. 3 as independent of $\bar{u}$. The minimum in H or H_{eff} appears because of the counteracting influence of the $B/\bar{u}$ term *versus* the high-velocity terms $C\bar{u}$ and $D\bar{u}$. When the pressure increases in Fig. 7a and b, $D_{1,2}$ becomes smaller, particularly at lower temperature (Fig. 6a). At the same time the k' values decrease with increasing pressure and, therefore, the factor C'' decreases (eqn. 7), whereas k_d increases (eqn. 8). As Fig. 7a and b show, the overall result is an increase in H_{eff} and a moving of its minimum, $H_{eff,min}$, to lower $\bar{u}$. When the temperature, instead of the pressure or density, is increased, as plotted in Fig. 8a and b, $D_{1,2}$ increases strongly, particularly at higher pressure (Fig. 6a). The k' values mostly decrease with increasing temperature in the temperature range investigated (Fig. 4). This leads to a similar behaviour of C'' and k_d, as before, with increasing pressure. As Fig. 8a and b show, the overall result with increasing temperature is an increase in H_{eff} at velocities around $\bar{u}_{opt}$ or lower in the plateau region, but a strong decrease in H_{eff} at higher velocities. Generally, a movement of $H_{eff,min}$ to higher $\bar{u}$ is observed at higher temperatures. The latter is just the opposite of the effect of increasing pressure in Fig. 7a and b.

ACKNOWLEDGEMENTS

We thank B. Lorenschat for able technical assistance and the Deutsche Forschungsgemeinschaft for financial support.

REFERENCES

1 S. T. Sie, W. van Beersum and G. W. A. Rijnders, *Sep. Sci.*, 1 (1966) 459.
2 S. T. Sie and G. W. A. Rijnders, *Sep. Sci.*, 2 (1967) 729.
3 S. T. Sie and G. W. A. Rijnders, *Sep. Sci.*, 2 (1967) 755.
4 M. Novotny, W. Bertsch and A. Zlatkis, *J. Chromatogr.*, 61 (1971) 17.
5 B. P. Semonian and L. B. Rogers, *J. Chromatogr. Sci.*, 16 (1978) 49.
6 J. E. Conaway, J. A. Graham and L. B. Rogers, *J. Chromatogr. Sci.*, 16 (1978) 102.
7 U. van Wasen, I. Swaid and G. M. Schneider, *Angew. Chem.*, 92 (1980) 585.
8 D. Leyendecker, F. P. Schmitz and E. Klesper, *J. Chromatogr.*, 315 (1984) 19.
9 F. P. Schmitz, D. Leyendecker and E. Klesper, *Ber. Bunsenges. Phys. Chem.*, 88 (1984) 912.
10 D. Leyendecker, F. P. Schmitz, D. Leyendecker and E. Klesper, *J. Chromatogr.*, 321 (1985) 273.
11 J. M. Levy and W. M. Ritchey, *J. High Resolut. Chromatogr. Chromatogr. Commun.*, 8 (1985) 503.
12 C. R. Yonker and R. D. Smith, *J. Chromatogr.*, 361 (1986) 25.
13 J. M. Levy and W. M. Ritchey, *J. Chromatogr. Sci.*, 24 (1986) 242.
14 B. W. Wright and R. D. Smith, *J. Chromatogr.*, 355 (1986) 367.
15 S. M. Fields, K. E. Markides and M. L. Lee, *J. Chromatogr.*, 406 (1987) 223.
16 C. R. Yonker, D. G. McMinn, B. W. Wright and R. D. Smith, *J. Chromatogr.*, 396 (1987) 19.
17 S. M. Fields, K. E. Markides and M. L. Lee, *J. High Resolut. Chromatogr. Chromatogr. Commun.*, 11 (1988) 25.
18 J. L. Venthey, J. L. Janicot, M. Caude and R. Rosset, *J. Chromatogr.*, 499 (1990) 637.
19 S. T. Sie and G. W. A. Rijnders, *Sep. Sci.*, 2 (1967) 699.
20 J. A. Graham and L. B. Rogers, *J. Chromatogr. Sci.*, 18 (1980) 75.
21 F. P. Schmitz, H. Hilgers, D. Leyendecker, B. Lorenschat, U. Setzer and E. Klesper, *J. High Resolut. Chromatogr. Chromatogr. Commun.*, 7 (1984) 590.
22 S. M. Fields and M. L. Lee, *J. Chromatogr.*, 349 (1985) 305.
23 R. C. Simpson, J. R. Gant and P. R. Brown, *J. Chromatogr.*, 371 (1986) 109.
24 D. R. Gere, R. Board and D. McManigill, *Anal. Chem.*, 54 (1982) 736.
25 S. Shah and L. T. Taylor, *Chromatographia*, 29 (1990) 453.
26 P. A. Mourier, M. H. Caude and R. H. Rosset, *Chromatographia*, 23 (1987) 21.
27 H. Engelhardt, A. Gross, R. Mertens and M. Petersen, *J. Chromatogr.*, 477 (1989) 169.
28 M. Ashraf-Khorassani, S. Shah and L. T. Taylor, *Anal. Chem.*, 62 (1990) 1173.
29 A. Hütz and E. Klesper, in preparation.
30 D. E. Martire, *J. Chromatogr.*, 461 (1989) 165.
31 H. J. Löffler, *Thermodynamische Eigenschaften binärer Gemische leichter gesättigter Kohlenwasserstoffe im kritischen Gebiet*, Verlag C. F. Müller, Karlsruhe, 1962.
32 *Zahlenwerte und Funktionen, Landolt–Börnstein*, Bd. 52 II, 1. Teil, 6. Auflage, Springer, Berlin, 1971, p. 167.
33 A. Hütz, D. Leyendecker, F. P. Schmitz and E. Klesper, *J. Chromatogr.*, 505 (1990) 99.
34 L. R. Snyder and J. J. Kirkland (Editors), *Introduction to Modern Liquid Chromatography*, Wiley, New York, 2nd ed., 1979.
35 E. Heftmann (Editor), *Chromatography, Fundamentals, and Application of Chromatographic and Electrophoretic Methods, part A: Fundamentals and Techniques (Journal of Chromatography Library*, Vol. 22A), Elsevier, Amsterdam, 1983.

36 H. G. Janssen, H. M. J. Snijders, J. A. Rijks, C. A. Cramers and P. J. Schoenmakers, *J. High Resolut. Chromatogr.*, 14 (1991) 439.
37 K. Stephan and K. Lucas, *Viscosity of Dense Fluids*, Plenum Press, New York, 1979.
38 R. C. Reid, J. M. Prausnitz and T. K. Sherwood (Editors), *The Properties of Gases and Liquids*, McGraw-Hill, New York, 3rd ed., 1977, p. 567.